19th Brazilian Congress of Thermal Sciences and Engineering
November 06th-10th, 2022, Bento Gonçalves - RS - Brazil

ENC-2022-0082
CONSTRUCTAL DESIGN AND RESPONSE SURFACE MODELING OF TUBE ARRANGEMENT HEAT EXCHANGER WITH TWO DEGREES OF FREEDOM FOR PSEUDOPLASTIC AND VISCOPLASTIC FLUIDS

Eduardo Henrique Taube Cunegatto
Marcelo Gotardo
Flávia Schwarz Franceschini Zinani
Mechanical Engineering Graduate Program, Universidade do Vale do Rio dos Sinos (UNISINOS). São Leopoldo, RS, Brazil.
eduardohtc@edu.unisinos.br
fonofico@edu.unisinos.br
fzinani@unisinos.br

Abstract. *In this work, the Constructal Design Method is applied to investigate tube arrangements for heat transfer with non-Newtonian fluids – pseudoplastic and viscoplastic – seeking the configuration that returns the maximum heat transfer density. Systems consisting of a row of tubes added by secondary tubes were analyzed, according to the Constructal Theory's hierarchy principle. In these systems, there are two degrees of freedom – the distance between the tubes and the tubes' diameter ratio. The systems were modeled and solved via Computational Fluid Dynamics (CFD), using the Power-Law and Bingham equations to predict the viscosity of pseudoplastic and viscoplastic fluids, respectively. The simulations were planned using Central Composite Designs, and the results were fitted using second order Response Surfaces. The results showed that the pseudoplastic fluids provide the highest heat transfer densities, due to the shear-thinning effect. Considering the three fluid models, the results showed that the heat transfer density is highly dependent on the two parameters (degrees of freedom) and that the interaction between the parameters is significant. The optimal configurations obtained differ considerably for each fluid – larger tubes and smaller spaces are beneficial to pseudoplastic fluids, while for viscoplastic, the opposite occurs.*

Keywords: *Constructal Design Method, Tube arrangements, Non-Newtonian Fluids, CFD, Optimization*

1. INTRODUCTION

Heat transfer equipment is present both in everyday applications and in industry, like in air conditioning, cooling, and refrigeration devices. This equipment exists from the microscale, as in the cooling of electronic components, to the mega-scale, such as boilers and water condensers in thermoelectric plants. The heat exchangers are designed to provide maximum heat exchange with the rational use of space and materials.

In industry, one of the most used heat exchanger models is the shell and tube type, in which a fluid flows inside the tubes and exchanges heat with another that flows outside them. This application motivates research on the flow around tube bundles. The complexity of this type of flow allows the investigation of configurations that have the potential to increase the performance of the device, with high sensitivity to operational conditions – types of fluids, flow regimes, temperatures, flow rates, etc.

Concerning the fluids used in industrial processes, they can be classified as Newtonian and non-Newtonian fluids. Non-Newtonian fluids have different rheological characteristics, among which the most common is the variable viscosity according to the deformations to which they are subjected. Pseudoplastic (or shear-thinning) fluids are among the most common non-Newtonian fluids. They are characterized by the reduction in apparent viscosity with increasing shear rates, that is, the thinning of the fluid as it is agitated or transported. Examples of pseudoplastic fluids are human blood, fruit pulp, sauces, paints, molten polymers, etc. (Chhabra and Richardson, 2008).

One can also relate to Non-Newtonian fluids another class of fluids: Viscoplastic or yield stress fluids. According to Barnes (2000), viscoplastic fluids exhibit a yield stress characteristic, that is, when subjected to the action of a force, they undergo "an abrupt and extreme change in behavior to a state of lower stress resistance". In practice, a fluid can be considered viscoplastic when, from given applied stress (the yield stress), it begins to behave similarly to a liquid fluid, which "will continue to deform without further increases in the applied stress". Therefore, below the yield stress

(characteristic of the material), it exhibits the behavior of a solid. Also, according to the author, several viscoplastic fluids can be found in everyday life. Among them, materials such as paints, toothpaste, food products, and even plastic explosives can be highlighted. In this way, there is a huge availability of exploitable materials whose results obtained within science can favor the productivity and yield of industries.

Among the methodologies used in the design of thermal systems, the Constructal Design method (CDM) has been consolidated in recent years. This has its origins in the Constructal Law, enunciated by Bejan (1997). The Constructal Law is related to the evolution of living systems, in which flows with different purposes are identified. According to Bejan and Zane (2012), the Constructal Law is stated as: "For a finite-sized flow system to persist in time (survive), its configuration must evolve in such a way that it provides more access to the easy to the currents that flow through it". The Construtal Law states that everything that moves, regardless of whether it is an animate (biological) or inanimate system, is a living system and that these systems evolve in a specific and deterministic direction (Bejan, 1997). In engineering projects, CDM defines objective functions, constraints, and degrees of freedom, in addition to prioritizing configurations with branching and hierarchy concepts, resulting in high-performance configurations, good distribution of imperfections, and low resistance to their flows. In 2005, a study was published on the performance of tube bundles configurations using the CDM method. In the article "Constructal multi-scale cylinders in cross-flow", Bello-Ochende and Bejan (2005) evaluated configurations of a row of tubes and configurations with secondary and tertiary tubes exchanging heat with air. Works by the research group NucREO (Group of rheology, flows and optimization) at UNISINOS, have been investigating tube bundles configurations with a view to better performance in heat exchange with non-Newtonian fluids using MDC. For example, the article by Klein, et al. (2017a) applied CDM in arrangements of elliptical section tubes, looking for configurations that maximize the heat transfer density for flows of pseudoplastic fluids, subject to the same pressure differential, represented dimensionally by the Bejan number. In this case, it was found that cylinders with an elongated section in the flow direction (slender) presented the best thermal exchange density, due to the greater shear and contact area of between cylinder and fluid, providing an increase in apparent viscosity and advective effects. The use of the Bejan number in the study of problems involving flows of non-Newtonian fluids subjected to pressure difference in tube bundles was examined by Klein, et al. (2017b). The authors presented a methodology for modeling non-Newtonian fluids, such as Power-Law, Carreau, and Bingham, together with a case study. The results show that the methodology allowed the evaluation of problems involving Non-Newtonian fluids from the point of view of Constructal Design. Hermany, et al. (2018) analyzed the optimal aspect ratio for elliptical tubes subjected to viscoplastic fluid flow. The authors concluded that low aspect ratios result in larger unyielded regions, which increase the heat transfer density. Razera, et al. (2019) evaluated the pitch and aspect ratio for elliptical tubes placed in a row, subjected to airflow, seeking the maximum heat transfer density settings. It was observed that the best performance was found for the highest aspect Ratio studied, , prevailing the principle of distribution of imperfections of the Constructal Design. Severo et al. (2021) studied Bingham fluid flow, for different Bejan numbers, in cylinders. It was noticed that the heat exchange density increases with the increase of the Bejan number and decreases with the increase of the minimum yield stress. Considering that the application of CDM in thermal systems involves the evaluation of geometric configurations, it becomes feasible to resort to Computational Fluid Dynamics (CFD) for the solution of flow and heat transfer problems. The use of this tool is very broad, provides results quickly and reliably, and becomes an alternative for reducing costs with experimentation (Maliska, 2004).

In most cases where the objective of investigation and design by MDC is to find an optimal configuration, it is common to work with optimization algorithms associated with MDC. In the case of using the exhaustive search, it may be necessary to carry out many simulations, which demands time and computational effort. Optimization methods might be employed to reduce the number of simulations and to provide more accurate results. One of the most used design modeling and optimization techniques is the Response Surface Methodology (RSM). This method consists of creating a metamodel from the results of simulations carried out according to a planned design. RSM uses the results of the simulations to create a regression model as a function of the studied parameters. Thus, the optimal result can be obtained from the response surface model developed by the regression of the experimental results – which, in the case of using CFD, are the results of the simulations (Rahmannezhad and Mirbozorgi, 2019).

Considering the above statement, this work aims, through the principles of the Constructal Law, through the MDC, to investigate the geometric effect and the best designs of tube bundles for heat transfer with pseudoplastic and viscoplastic fluids. The proposed configuration follows the two degrees of freedom model introduced by Bello-Ochende and Bejan (2005), characterized by the evolution of the main system, through the addition of secondary cylinders, which presented successful results for Newtonian fluid flow (air). RSM is used for planning the cases, which are solved by CFD, as well as for data regression, analysis of effects, and obtaining the optimal points, i.e., geometries that maximize heat transfer.

2. METHODOLOGY

2.1 Constructal Design

The application of the Construtal Design method follows a step-by-step scheme, based on the work of Rocha, et al. (2017) and Dutra et al. (2021). In general, this methodology presupposes the definition of a finite-size system, the

identification of the flow that, when facilitated, causes better system performance, the definition of a performance indicator, the definition of restrictions and degrees of freedom, the evaluation of settings, and a method for identifying the best performing settings.

Step 1: System definition

The system used in the present study is schematized in Figure 1. The model represents the forced convection of a non-Newtonian fluid over a row of cylindrical tubes. All cylinders have a constant surface temperature, T_w, and the fluid enters the domain at a temperature equal to T_0. The flow is driven by the pressure differential ΔP. The main tube has fixed diameter D_0 and downstream distances, L_d, and upstream, L_u, defined by $50D_0$ and $6D_0$, respectively, and the secondary tubes have variable radius R_1. The system, from the point of view of thermal analysis, is given by the hatched region of Figure 1, which is based on the hypothesis of symmetry in the dashed lines.

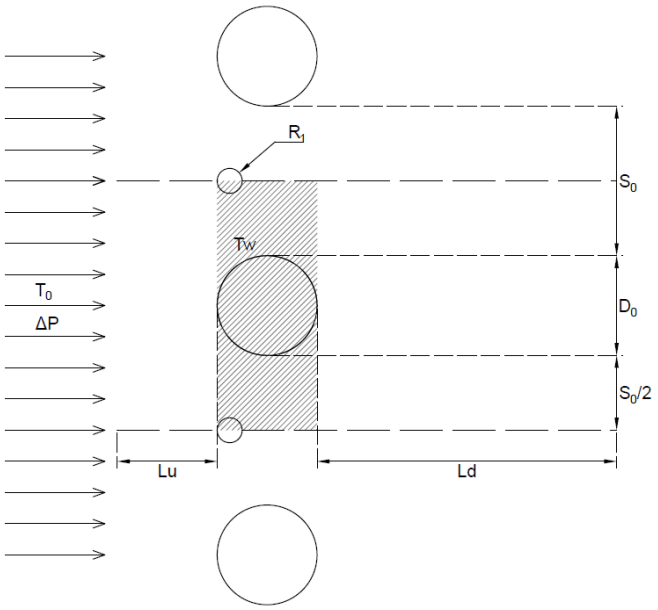

Figure 1. Scheme representing the physical system.

Step 2: Identification of the flow

In this system, the fluid flows over the tubes. However, in the Constructal Design Method, this step identifies what flows are related to the purpose of the system. In this case, the purpose of the system is to transfer heat, so the focus of the method is on the heat flow from the tubes.

Step 3: Definition of the performance indicator

The performance indicator used to evaluate geometries is the heat transfer rate. As it is desired to increase the heat transfer rate for a constant volume, the dimensionless heat transfer density, Q^*, defined by Equation 1, is used as a performance indicator for the CDM.

$$Q^* = \frac{q' D_0}{D_0(D_0+S_0)\kappa(T_w-T_0)} \tag{1}$$

where q' is the rate of heat transfer from the tube walls and κ is the thermal conductivity of the fluid.

Step 4: Degrees of Freedom

The degrees of freedom to vary the system configuration to achieve the best performance are the distance S_0 and the radius of the secondary cylinders, R_1. Dimensionally, both parameters are represented, respectively, by S_0/D_0 and R_1/D_0.

Step 5: Restrictions

As previously mentioned, the restriction imposed is the volume of the system, given by the hatched region in Figure 1, in addition to the geometric physical restrictions related to the non-overlapping of the cylinders. With constraints delimited, we set the initial search space to the best settings:

$0.20 < S_0/D_0 < 1.00$

$0.05 < R_1/D_0 < 0.15$

Step 6: Design of Experiments and Response Surface Methodology

The experimental (simulation) design (DOE) was carried out using the Central Composite Design (CCD) method (Montgomery, 2012), through the *R Statistic* programming language, via the *RStudio* programming environment. For this, the delimited restrictions were used to create the initial screening space, as shown in Table 1. With the application of the CCD, geometric configurations are generated in which simulations are carried out to determine a database for the application of the Response Surface Methodology (RSM).

Table 1. Configuration of variables to determine the screening space.

Variable	Levels				
	Low Axial Level	**Low 2^k Level**	**Central Level**	**High 2^k Level**	**High Axial Level**
S_0* [m]	0.2	0.317	0.6	0.883	1
R_1* [m]	0.05	0.065	0.1	0.135	0.15

As the database is obtained, surfaces are generated by the RSM method, and through them, the point of best performance, which is predicted by the mathematical model described by Equation 2, is identified in the screening space. From this, a new reduced screening space is created, around this point, and is used as the Central Level for the application of a new CCD. From this, a new dataset is generated, along with a new surface, and the data from the previous CCD is discarded. Again, the best performance point of this last model is identified, and a new cycle is repeated until the identified maximum has a small difference compared to the last one.

$$Q^* = \beta_0 + \beta_1 S_0^* + \beta_2 R_1^* + \beta_3 S_0^* R_1^* + \beta_4 {S_0^*}^2 + \beta_5 {R_1^*}^2 \tag{2}$$

where S_0* and R_1* represents the independent variable(s), Q* the response variable, β the regression coefficients. The regression coefficients are determined by the method of least squares, represented by:

$$Q^* = X\beta = \begin{bmatrix} {Q^*}_1 \\ {Q^*}_2 \\ \vdots \\ {Q^*}_n \end{bmatrix} = \begin{bmatrix} 1 & {R^*}_{1_1} & {S^*}_{0_1} \\ 1 & {R^*}_{1_2} & {S^*}_{0_2} \\ 1 & \vdots & \vdots \\ 1 & {R^*}_{1_n} & {S^*}_{0_n} \end{bmatrix} . \begin{bmatrix} \beta_0 \\ \beta_1 \\ \vdots \\ \beta_n \end{bmatrix} \tag{3}$$

$$X^T Q^* = X^T X\beta \tag{4}$$

$$(X^T X)^{-1} X^T Q^* = (X^T X)^{-1} X^T X\beta = \beta \tag{5}$$

where X represents the matrix of independent variables, and the superscript T represents the transposition of the matrix (Washington, 2011).

Before defining an acceptable model, all functions undergo a statistical analysis, to verify fit and precision, through the *MAE* (mean absolute error) parameters, which represent the absolute difference between the simulated result and the value predicted by the model, and R^2 (coefficient of determination), which determines how well the model fits the simulated results (El Hami, Pougnet, 2020). It was determined that, for a model to be considered satisfactory, the *MAE* value must be less than 1% of the maximum value and the R^2 value must be equal to or greater than 90%. The values of R^2 and *MAE* are calculated, respectively, by:

$$R^2 = 1 - \frac{\sum_{i=1}^{m} \left(Q^*_{sim_i} - Q^*_{model_i} \right)^2}{\sum_{i=1}^{m} \left(Q^*_{sim_i} - \overline{Q^*_{sim}} \right)^2} \tag{6}$$

$$MAE = \frac{\sum_{i=1}^{m} |Q^*_{model_i} - Q^*_{sim_i}|}{m} \tag{7}$$

where Q* represents the heat exchange density (response variable), and the subscripts *model* and *sim* represent the values predicted by the regression model and the simulation values, respectively; m represents the number of simulation data used to build the model. The bar in the denominator of Equation 6 indicates the mean value of the variable in question.

Step 7: Simulations

The determination of heat transfer density for each DOE simulation was performed using Computational Fluid Dynamics (CFD).

2.2 Mathematical Modelling

The mathematical modeling of the problem of flow and heat transfer around the tubes, in the two-dimensional domain consisting of the fluid region shown in Figure 1, is given by the steady-state equations of mass, momentum, and energy balances for incompressible non-Newtonian fluids. Dimensionless, these equations are described as:

$$\frac{\partial u^*}{\partial x^*} + \frac{\partial v^*}{\partial y^*} = 0 \tag{8}$$

$$\frac{Be}{Pr}\left(u^* \frac{\partial u^*}{\partial x^*} + v^* \frac{\partial u^*}{\partial y^*}\right) = -\frac{\partial P^*}{\partial x^*} + \eta^* \nabla^2 u^* \tag{9}$$

$$Pr\left(u^* \frac{\partial T^*}{\partial x^*} + v^* \frac{\partial T^*}{\partial y^*}\right) = \nabla^2 T^* \tag{10}$$

where ∇^2 is the tensor field, Be is the dimensionless Bejan number and Pr is the dimensionless Prandtl number, represented respectively by:

$$\nabla^2 = \frac{\partial^2}{\partial x^{*2}} + \frac{\partial^2}{\partial y^{*2}} \tag{11}$$

$$Be = \frac{\Delta P D_0^2}{\eta_c \alpha};\ Pr = \frac{\eta_c}{\rho \alpha} \tag{12}$$

The dimensionless form for position, velocity, pressure, temperature, and viscosity are defined, respectively, by Equation 13, and the other geometric variables of the problem, are represented by Equation 14:

$$(x^*, y^*) = \frac{x,y}{D_0};\ (u^*, v^*) = \frac{u,v}{\frac{\Delta P D_0}{\eta_c}};\ P^* = \frac{P}{\Delta P};\ T^* = \frac{T - T_0}{T_0 - T_w};\ \eta^* = \frac{\eta(\dot{\gamma})}{\eta_c} \tag{13}$$

$$(L_u^*, L_d^*, R_1^*, S_0^*) = \frac{L_u, L_d, R_1, S_0}{D_0} \tag{14}$$

The parameter η_c represents the characteristic viscosity of a Non-Newtonian fluid. Unlike Newtonian fluids, whose viscosity presents a linear behavior when subjected to shear stress, in Non-Newtonian fluids, viscosity is a function of the characteristic shear rate, represented by $\dot{\gamma}_c$ (Chhabra and Richardson, 2008). Based on this, the characteristic viscosity and characteristic shear rate are defined, respectively, by:

$$\eta_c = \eta(\dot{\gamma}_c);\ \dot{\gamma}_c = \sqrt{\frac{\Delta P}{\rho D_0^2}} \tag{15}$$

To define the viscosity function of pseudoplastic fluids, represented in Equation 15, the Ostwald-de-Waele rheological model, better known as the Power Law model, was used (Chhabra and Richardson, 2008):

$$\eta_c = K \dot{\gamma}_c^{n-1};\ \eta(\dot{\gamma}) = K \dot{\gamma}^{n-1} \tag{16}$$

where *K* is the fluid consistency index, *n* is the fluid behavior index and $\dot{\gamma}$ is the shear rate. For Newtonian fluids, the value of *n* is equal to 1 (one). If the value of *n* is less than one, the fluid will have a *shear-thinning* behavior, that is, the greater the shear rate on the fluid, the less viscous it becomes.

Concerning viscoplastic fluids, in turn, their viscosity can be represented with the modified Herschel-Bulkley model represented by Equation 17, as well as the dimensionless Bingham number:

$$\eta(\dot{\gamma}) = \begin{cases} \frac{\tau_0}{\dot{\gamma}} + K \mid \dot{\gamma} > \dot{\gamma}_{crit} \\ \frac{\tau_0\left(2 - \frac{\dot{\gamma}}{\dot{\gamma}_{crit}}\right)}{\dot{\gamma}_{crit}} \mid \gamma < \dot{\gamma}_{crit} \end{cases};\ Bn = \frac{\tau_0}{\dot{\gamma}_c \eta_c} \tag{17}$$

where τ_0 is the yield stress, $\dot{\gamma}_{crit}$ is the critical shear rate and Bn is the dimensionless Bingham number. For Newtonian fluids, the value of Bn is equal to 0 (zero). However, the greater the Bn, the greater the value assumed by τ_0, and greater shear stress must be applied to start the fluid flow. Otherwise, the fluid will behave like a solid material. The critical shear

rate, in turn, is a rheological parameter for viscosity adjustment and was determined from the analysis of the variation in heat exchange density.

Concerning the boundary conditions, the static pressure of value ΔP and temperature T_0 on the western face (inlet) were used; symmetry condition on the northern and southern faces; static pressure equal to zero on the eastern face (outlet); non-slip wall condition and temperature T_w at the cylinder walls.

2.3 Numerical Methodology

To solve the governing equations described in the previous section, the ANSYS FLUENT 2021 R2 algorithm was used, which uses the Finite Volumes method (PATANKAR, 1984). The pressure-velocity coupling used was Coupled, and second-order interpolation functions were used for pressure, moment, and energy, as well as double-precision, was used for all calculations. The convergence criteria used were 10^{-6} for continuity and momentum and 10^{-8} for energy. Relaxation factors used were 0.5 for pressure and moment and 0.75 for energy.

3. RESULTS

The problem studied in this work was performed with flows of fixed Pr number equal to 5, Be number equal to $10^{5,}$ and Power-Law indices of values 0.5 for pseudoplastic fluid, 1 for Newtonian fluid, and Bn number equal to 2 for viscoplastic fluid. The geometric variations and other parameters of each case were determined in the previous sections.

The geometry has two degrees of freedom: spacing between cylinders (S_0*) and the radius of the intermediate cylinder (R_1*), which represent the independent variables of the problem, and the independent variable is the heat transfer density (Q*). As a result, the response surfaces show the variation of Q* as a function of the other variables, in the form of a projection and a three-dimensional graph, as shown in Figure 2.

The projected surface of Figure 2 allows the visualization of the behavior of Q* throughout the screening space. It is important to point out that the scales of each surface are different due to the maximum region identified through the methodology used. Each line represents a range of values, and the colors indicate the intensity: the brighter, the higher the Q* value. For all cases, it was possible to determine a surface that presents a well-defined maximum region, allowing the determination of the configuration that best presents the global thermal performance. The three-dimensional graph in Figure 2 serves as a complement to the projection version and it allows the visualization of the gradients of each variable, as well as the behavior of the response surface. The maximum region is represented by the domes (peaks) in the region of optimal configuration and decreases as the parameters move from the ideal values, as expected.

Observing the surfaces (a) of Figure 2, referring to the pseudoplastic fluid (n = 0.5), it is noted that R_1* has a great influence on the behavior of Q*, especially when the radius increases from the maximum point. The S_0* spacing does not have such a significant impact locally, since the variation of Q* for a fixed value of R_1* is smaller. However, it is important to reiterate that the values of S_0* are smaller compared to the other cases, and it is estimated that, for larger S_0*, the impact of this is greater.

Regarding the surfaces (b) of Figure 2, referring to the Newtonian fluid (n = 1), it can be seen that the influence of both geometric parameters is significant, since Q* changes for any change in geometry, even for a small margin, due to the reduced screening space. However, even if the variation of Q* is small, it is enough to show the behavior of the response variable as the geometry changes.

Finally, the surfaces (c) of Figure 2, which represent the viscoplastic fluid (Bn = 2), indicate a behavior opposite to the pseudoplastic fluids, that is, the S_0* spacing has a great influence on the response, while R_1* has a smaller impact. In this case, Q* values obtained were lower than for the previous fluids and the geometric variation, and the geometry presents the highest optimal S_0* and an optimal R_1* equivalent to the Newtonian fluid.

The surfaces obtained in Figure 2 were built using polynomial mathematical models that follow the form described by Equation 2. Therefore, the data obtained by the simulations were necessary to calculate the coefficients of each case (Eqs. 3, 4, and 5), generating a specific equation for each surface. The evaluation of the models was performed as described in the Methodology section, via parameters R^2 and *MAE* (Eqs. 6 and 7). The evaluation can also be done graphically via *fit plots*, which compare the values predicted by the model and the simulated values, as shown in Figure 3.

In the graphs of Figure 3, the red dots represent the values predicted by the model, while the line represents the real values. With this, it is possible to see how much the model fits with the real data. Regarding the R^2 parameter, its visual interpretation is simple: the closer the points are to the line, the better the fit and, therefore, the higher its value. The *MAE* parameter represents the average of the sum of the "distances" of the points in relation to the line, that is, the average of the sum of the differences between the predicted values and the simulated values. Therefore, the smaller this distance, the smaller the *MAE* value. It can also be seen, through the data in Figure 3, that the satisfaction criteria went far beyond what was expected, allowing the achievement of models that can predict above 98% of the response variation, as shown by the R^2 values. Furthermore, the *MAE* values indicate that the models can predict values with a difference of approximately $\mp$0.18% for the pseudoplastic fluid, $\mp$0.03% for Newtonian fluid, and $\mp$0.12% for viscoplastic fluid compared to the respective optimal values. Table 2 presents the optimal values.

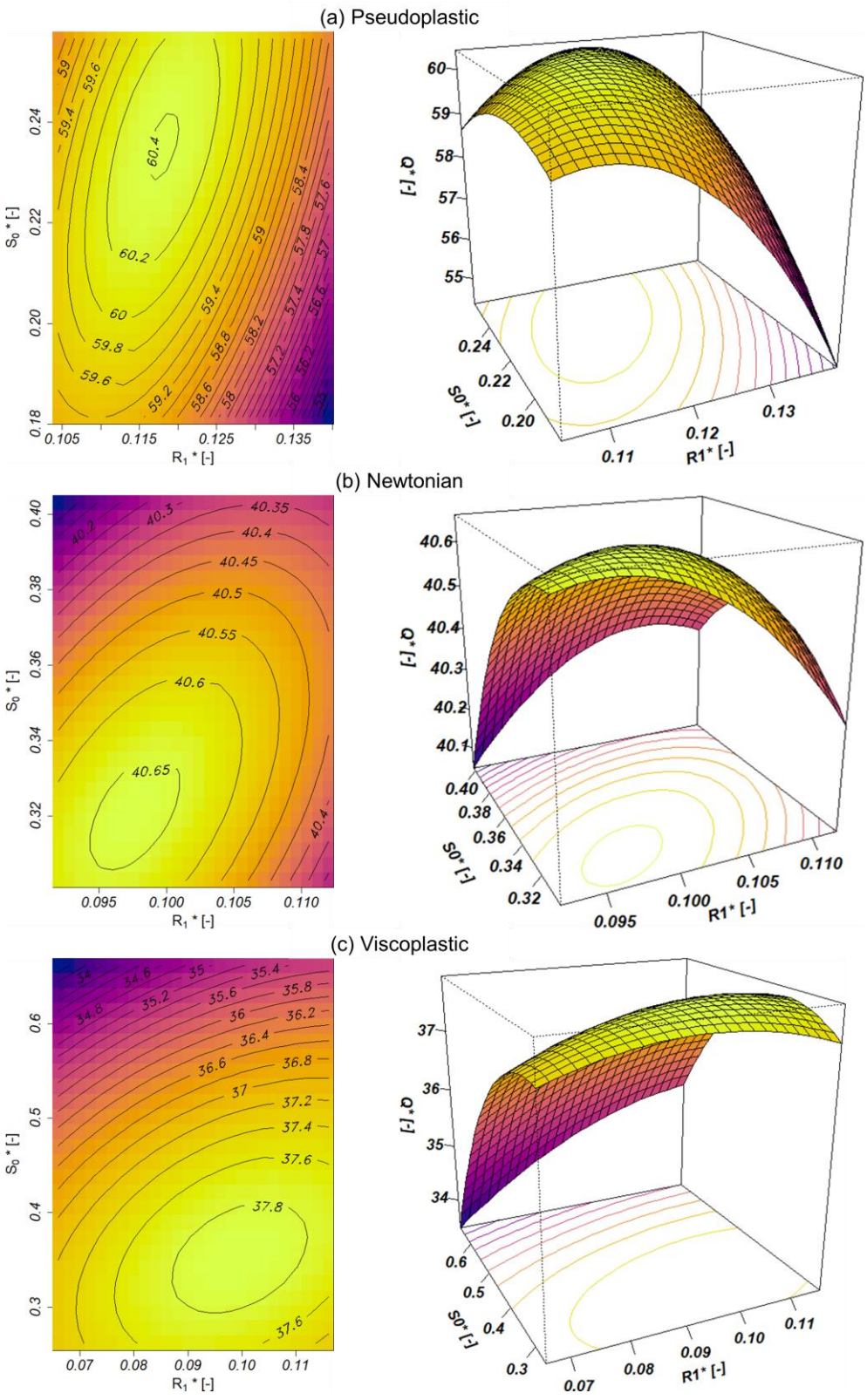

Figure 2. Three-dimensional response surfaces (right) and projection (left) for each fluid: (a) Pseudoplastic; (b) Newtonian; (c) Viscoplastic.

As already shown in Figure 2, Q^*_{max} decreases as the flow index value increases, that is, n = 0.5 for pseudoplastic fluid and n = 1 for a Newtonian fluid. This increase is mainly associated with rheological differences between such fluids. As seen in the previous sections, pseudoplastic fluids benefit from the *shear-thinning* effect, causing the viscosity to decrease under shear stress. Consequently, the fluid offers less resistance to flow, facilitating the transport of properties.

Furthermore, the low value of $S_0{}^*_{,opt}$ contributes to a high heat exchange density. On the other hand, the difference in Q^*_{max} between Newtonian and viscoplastic fluids, more specifically Bn = 2, is not so pronounced, and it is also clear that the optimal geometry for such cases is also similar. To observe the effects of flow under optimal conditions, Figure 4 presents streamlines (upper) and temperature fields (lower) in the optimal configuration of each fluid. For viscoplastic fluid, the strain rate field is also presented.

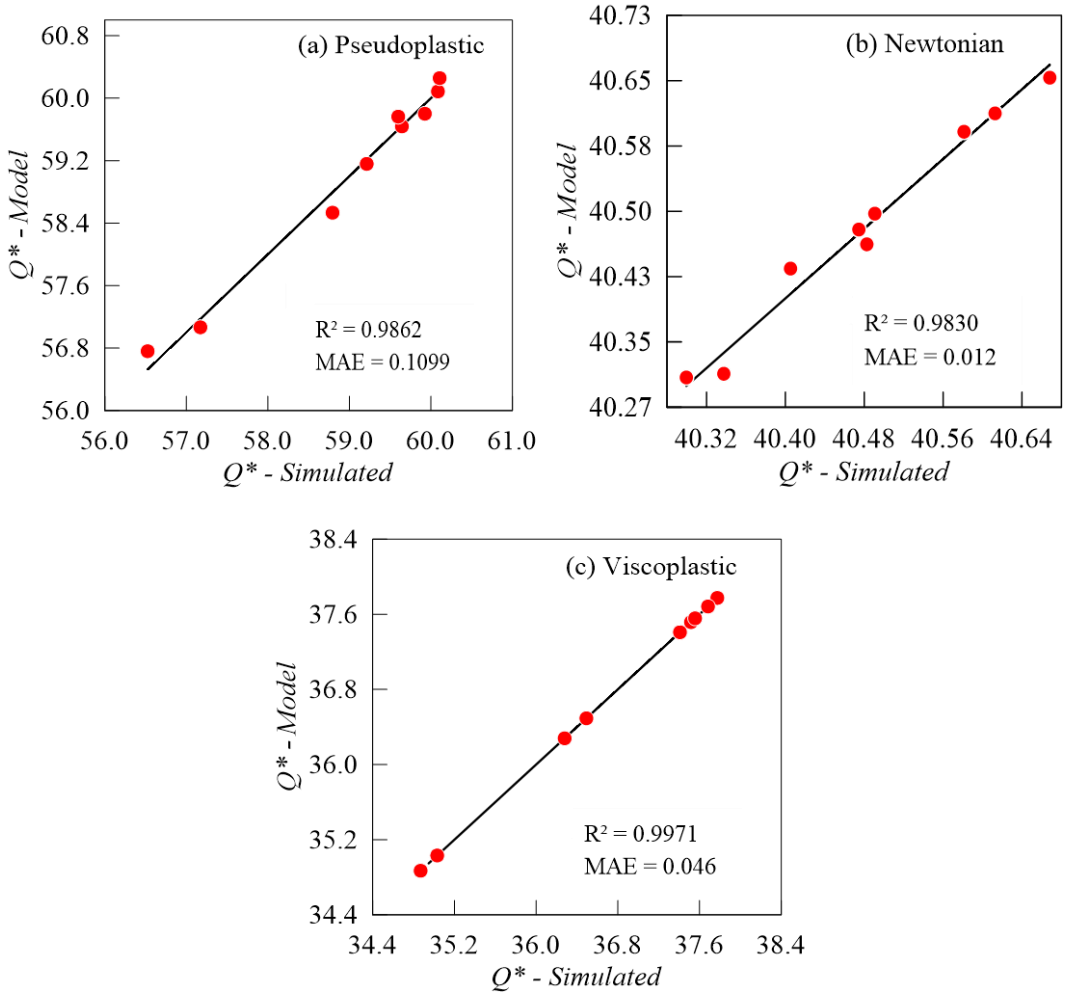

Figure 3. Fit plots of the mathematical models of each fluid: (a) Pseudoplastic; (b) Newtonian; (c) Viscoplastic.

Table 1. Optimal configurations and maximum responses for each fluid.

Fluid	$S_0{}^*_{,opt}$	$R_1{}^*_{,opt}$	$Q^*_{max,\ model}$	$Q^*_{max,\ exp}$	Diff
Pseudoplastic	0.235	0.118	60.267	60.417	0.25%
Newtonian	0.321	0.098	40.661	40.659	0.01%
Viscoplastic	0.352	0.100	37.884	38.059	0.46%

Analyzing Figure 4, attention is drawn to the wakes downstream of the main cylinder, shown by streamlines, as they are a characteristic of flows over cylinders. As stated in the previous paragraph, pseudoplastic fluids offer less resistance to flow and, therefore, flow more easily, so that the flow separates, practically in the middle of the cylinder, causing a larger wake region. The presence of a larger wake region contributes to the thermal exchange, due to the mixing between the fluid particles. Another factor that contributes to the better performance of pseudoplastic fluids is a thinner thermal boundary layer. This means that the temperature gradients occur in a smaller space, allowing $S_0{}^*_{,opt}$ to be smaller. It also allows $R_1{}^*_{,opt}$ to be larger, without the thermal boundary layers influencing each other negatively, thus increasing the heat transfer area. In terms of heat exchange density, this effect is extremely beneficial because, since the performance indicator is restricted to a fixed volume, a lower value of $S_0{}^*$ leads to an increase in Q^*. As for Newtonian fluids, $S_0{}^*_{,opt}$ increases significantly and Q^* decreases. Since Newtonian fluids do not benefit from any effect regarding the reduction of viscosity, they require a bigger space to flow, as their thermal boundary layer seems larger than that of pseudoplastic

fluids. It is possible to notice from the streamlines that the Newtonian flow detaches from the cylinder in its back, originating smaller wakes. Lastly, viscoplastic fluid has the smallest wake region compared to the other analyzed fluids. However, the region of the wake is characterized as a region of high viscosity and consequently, it tends to be a zone of low velocity. This effect can be explained by the rheological behavior of this type of fluid, since, unlike the others, it needs a minimum stress to flow. Given this, the analysis can be carried out considering yielded/unyielded contours based on the critical shear rate, as the black region represents an unyielded flow, that is, a region of high viscosity, while the white region represents the yielded flow. In this case, it can be seen that the fluid will deform to the point that it ends up yielding due to the shear stress caused by contact with the cylinders. This creates a region of high strain rate which is compensated by a reduction in the viscosity. Henceforth, the heat transfer density is improved, since the fluid offers less resistance, augmenting the advective effects in that zone.

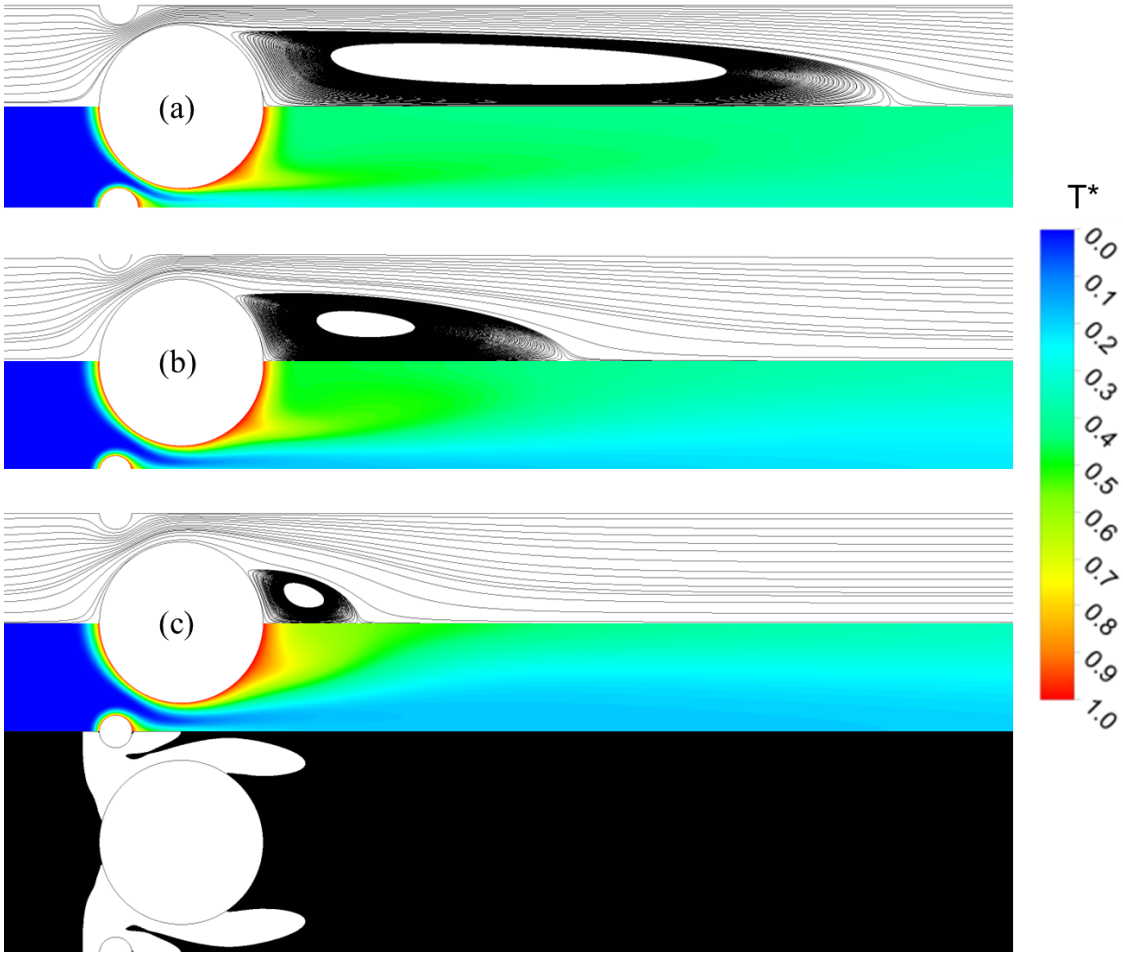

Figure 4. Streamlines (upper) and temperature fields (lower) in the optimal configuration of each fluid: (a) Pseudoplastic; (b) Newtonian; (c) Viscoplastic - strain rate field at the bottom of temperature field.

4. FINAL REMARKS

In the present work, flows of Newtonian, pseudoplastic and viscoplastic fluids around a tube row heat exchangers were evaluated. Applying the principles of the Construtal Law, through the Constructal Design Method, combined with the Response Surface methodology, it was possible to identify geometric configurations that would achieve the best performance in terms of heat transfer density. Through the response surfaces, which originated from high-reliability mathematical models, it was possible to identify the region that best fits the performance indicator, as well as to observe its behavior when the geometry changes. It was observed that the best performance was obtained by pseudoplastic fluid, due to its rheological characteristics, which provide more freedom for the geometry to evolve, resulting in a configuration with a lower volume for heat transfer. As the fluid becomes more viscous, the flow needs more space (larger S_0* and smaller R_1*) to optimize heat exchange, which reduces performance in terms of heat transfer density.

5. ACKNOWLEDGEMENTS

This work was funded by CAPES, CNPq and FAPERGS. E.H.T. Cunegatto is a CAPES scholarship holder (Code 001). M. Gotardo is a CNPq scholarship holder. F. Zinani is a grant holder of CNPq (Proc. No. 311444/2021-0). The project was funded by FAPERGS via the PqG public notice (Proc. No. 21/2551-0002169-1).

6. REFERENCES

Barnes, H. A. *A handbook of elementary rheology*. University of Wales: Institute of Non-Newtonian Fluid Mechanics, Aberystwyth, 2000.

Bejan, A. Constructal-theory network of conducting paths for cooling a heat generating volume. *International Journal of Heat and Mass Transfer*, v. 40, p. 799-816, 1997.

Bello-Ochende, T.; Bejan, A. Constructal multi-scale cylinders in cross-flow. *International Journal of Heat and Mass Transfer*, v. 48, p. 1373-1383, 2005.

Chhabra, R. P.; Richardson, J. F. *Non-Newtonian Flow and Applied Rheology*. Butterworth-Heinemann, Oxford, 2008.

Dutra, R. F; Zinani, F.S.F; Rocha, L.A.O; Biserni, C. Effect of non-Newtonian fluid rheology on an arterial bypass graft: A numerical investigation guided by constructal design. *Computer Methods and Programs in Biomedicine*, v. 201, 2021.

El Hami, A; Pougnet, P. *Embedded Mechatronic Systems 2: Analysis of Failures, Modeling, Simulation and Optimization*. 2. Ed. London: ISTE Press, 2020.

Frost, J. *Regression Analysis, An intuitive guide for using and interpreting linear models*. Statistics By Jim Publishing, 2019.

Hermany, L.; Lorenzini, G.; Klein, R.J.; Zinani, F.F.; Dos Santos, E.D.; Isoldi, L.A.; Rocha, L.A.O. Constructal design applied to elliptic tubes in convective heat transfer cross-flow of viscoplastic fluids. *International Journal of Heat and Mass Transfer*, v. 116, p. 1054-1063, 2018.

Klein, R.J.; Lorenzini, G.; Zinani, F.S.F.; Rocha, L.A.O. Dimensionless pressure drop number for non-Newtonian fluids analysis to Constructal Design of heat exchangers. *International Journal of Heat and Mass Transfer*, v. 115, p. 910-914, 2017 a.

Klein, R.J.; Biserni, C.; Zinani, F.S.F.; Rocha, L.A.O. Constructal design of tube arrangements for heat transfer to non-Newtonian fluids. *International Journal of Mechanical Sciences*, v. 133, p. 590-597, 2017 b.

Maliska, C.R. *Transferência de Calor e Mecânica dos Fluidos Computacional*. 2. Ed. Rio de Janeiro: LTC, 2004.

Montgomery, D.C. *Design and Analysis of Experiments*, 8. Ed., John Wiley & Sons, New Jersey, 2012.

Patankar, S. V. *Numerical Heat Transfer and Fluid Flow*. McGraw-Hill, New York, 1980.

Rahmannezhad.J.; Mirbozorgi, S.A. CFD analysis and RSM-based design optimization of novel grooved micromixers with obstructions, *International Journal of Heat and Mass Transfer*, v. 140, p. 483-497, 2019.

Razera, A.L.; Quezada, L.A.; Fagundes, T.M.; Isoldi, L.A.; Dos Santos, E.D.; Biserni, C.; Rocha, L.A.O, Fluid flow and heat transfer maximization of elliptic cross-section tubes exposed to forced convection: A Numerical approach motivated by Bejan's theory. *International Communications in Heat and Mass Transfer*, v. 109, 2019.

Rocha, L.A.O; Lorente, S; Bejan, A. Constructal Theory in Heat Transfer. In: *Handbook of Thermal Science and Engineering.* [S.1]: Springer, p. 329-370, 2017.

Severo, L.F.; Zinani, F.F.; Rocha, L.A.O. Constructal design analysis of viscoplastic cross-flow over a row of cylinders. *International Communications in Heat and Mass Transfer*, v. 122, 2021.

Washington, S.P.; Karlaftis, M.G.; Mannering, F.L. *Statistical and Econometric Methods for Transportation Data Analysis*, 2. Ed., Chapman & Hall/CRC, 2011.

7. RESPONSIBILITY NOTICE

The authors are the only ones responsible for the printed material included in this paper.